Numerical simulation of concrete structure affected by AAR: the case study of Kariba dam

Esposito, Rita; Hendriks, Max; Lilliu, G; Schreppers, G.M.A

Publication date
2011

Document Version
Accepted author manuscript

Published in
XI Icold benchmark workshop on numerical analysis of dams

XI ICOLD BENCHMARK WORKSHOP ON NUMERICAL ANALYSIS OF DAMS
Valencia, October 20-21, 2011

THEMA A

NUMERICAL SIMULATION OF CONCRETE STRUCTURE AFFECTED BY AAR: THE CASE STUDY OF KARIBA DAM

Esposito, Rita[1]

Handriks, Max A.N.[2]

Lilliu, Giovanna[3]

Schreppers, Gerd-Jan M.A.[4]

CONTACT

MSc Rita Esposito, Delft University of Technology, Department of Structural Mechanics, Stevinweg 1 (2628 CN, Delft, The Netherlands), +31 (0)15 27 82537 r.esposito@tudelft.nl.

Summary

The durability of concrete structures and infrastructures is a relevant topic for civil engineers. It can comprise long-term effects including chemical reactions, which produce concrete swelling.

The Kariba arch dam is a representative case study to investigate the swelling phenomenon in concrete structures due to Alkali-Aggregate Reaction (AAR). For the 11th ICOLD Benchmark Workshop, the dam is analyzed with a modified version of the DIANA Finite Element program.

The AAR damages are evaluated with a thermo-chemo-mechanical model based on an approach by Ulm et al [1]. The Larive's law [2] is adopted to define the AAR expansion evolution in function of time. The influence of imposed stress on orthotropic chemical strains is also taken in account, as suggested by Saouma and Perotti [3]. A comparison with a straightforward method is also shown to underline the relevance of the stress state on the swelling phenomenon.

[1] Delft University of Technology, Department of Structural Mechanics, Delft, The Netherlands.
[2] Delft University of Technology, Department of Structural Mechanics, Delft, The Netherlands.
[3] TNO DIANA BV, Delft, The Netherlands.
[4] TNO DIANA BV, Delft, The Netherlands.

1. Introduction

The Kariba dam is an example of AAR-affected concrete structure, already object of many ICOLD conferences, it is proposed for the 11th Benchmark Workshop on Numerical Analysis of Dams.

It is a long double curvature arch dam built across the Zambezi River between 1956 and 1959. The dam shown evident signs of swelling soon after the starting of its operation; for this reason many instruments are placed over the years to monitor its behavior.

In this paper the dam is analyzed with a modified version of the DIANA software. A 3D mesh is defined and interface elements are placed between the dam and the foundation. An elastic behavior is considered for concrete and soil. A thermo-chemo-mechanical model, on the basis of Ulm's model [1], is implemented in the standard DIANA code. The model takes in account the effect of the stress state on the orthotropic swelling, according to Saouma and Perotti [3]. In order to fit the experimental results, the parameters of Larive's kinetic law [2] are calibrated. The relevance of the stress influence on this calibration is underlined adopting a straightforward analysis with fixed and predefined orthotropic swelling.

2. Adopted model

2.1. Finite Element Model

Quadratic brick elements with 3x3x3 integration schema are adopted to model the dam and the foundation (Figure 1). The contact between the two components is modeled with quadratic interface elements with a Newton-Cotes integration scheme with 3x3 integration points. The mesh is based on the second mesh proposed in the Benchmark Guidelines [4].

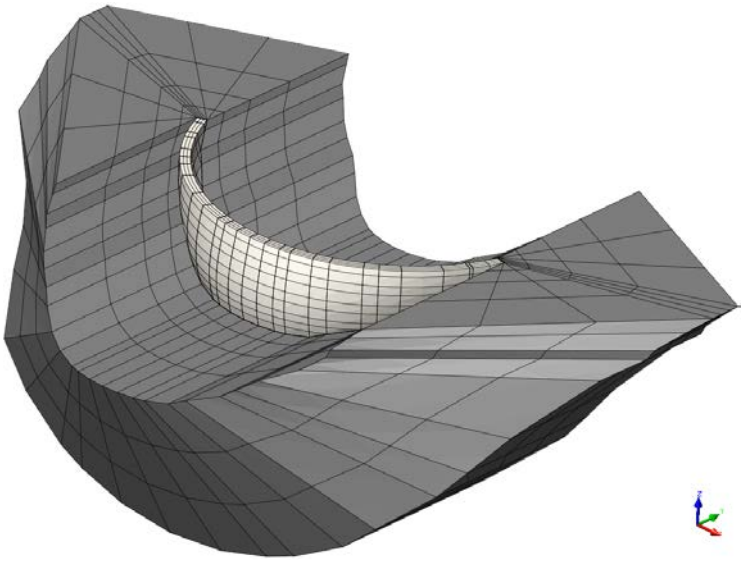

Figure 1: Finite elements mesh [4].

In order to simulate the construction and operation periods of the dam, a phased analysis is adopted. In the first phase the cantilevers are physically and topologically isolated and the dead weight is applied. The stress situation of this phase is included as initial stress in the second phase of the analysis, omitting the displacements. During the operation period (1962-2010), rigid tying elements are used connecting the cantilevers.

Due to the location of the dam, a small temperature variation around 27 °C is observed during the year; for this reason the thermal effect are not included in the analysis.

As proposed in the Benchmark Guidelines [4], the water pressure is considered constant during four subsequent periods. The four main levels are given in Table 1.

Table 1: Applied water level.

Period	Water level
1962-1973	483.80 m
1974-1981	486.10 m
1982-1995	479.90 m
1995-2010	483.00 m

2.2. Material model

The concrete and the soil are modeled linearly elastic; their mechanical characteristics are given in Table 2, according to the Benchmark Guidelines [4].

Table 2: Mechanical properties of concrete and soil.

Property	Unit	Foundation rock	Dam concrete
Elastic modulus	N/m^2	$1.0\ 10^7$	$2.2\ 10^7$
Poisson's ratio	-	0.2	0.2
Unit weight	N/m^3	Not considered	$2.35\ 10^3$

Nonlinear interface elements are placed between dam and its foundation. In the normal direction the elastic stiffness is set to 10^{11} N/m^3 in compression and 10^3 N/m^3 in tension, that is, stiff in compression and nearly stress free in tension. In the shear direction the stiffness is constant and equal to 10^{10} N/m^3

The chemical aspect of AAR is included in the model through the Larive's formulation [2].

$$\varepsilon^{vol} = \varepsilon_{\infty} \frac{1-\exp(-t/t_c)}{1+\exp\left(\frac{t_l - t}{t_c}\right)} \tag{1}$$

where ε_{∞} is the asymptotic volumetric expansion, t_l and t_c are the latency and characteristic time, respectively.

In Figure 2 and Table 3 the adopted kinetic law and the selected parameters are given. It is assumed that the expansion starts immediately after the impounding, in 1963.

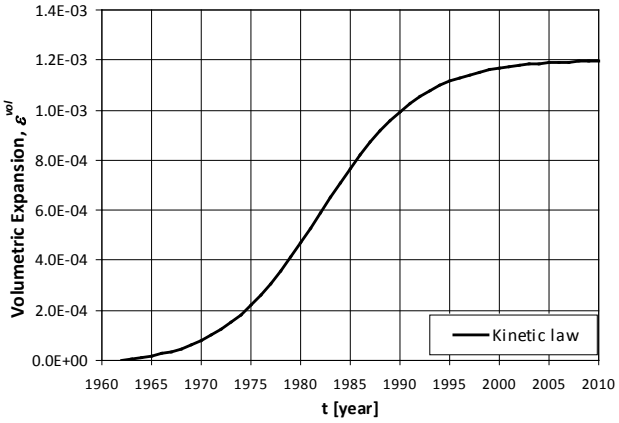

Figure 2: Adopted kinetic law.

Table 3: Parameters of the kinetic law.

Parameter	Value
Asymptotic expansion ε_∞	0.12 %
Latency time t_l	20 year
Characteristic time t_c	5 year

The kinetic law is calibrated including the "expansion transfer" concept. As shown from Multon and Toutelemonde [5], the volumetric strain due to AAR swelling can be redistributed on the basis of the principal stresses. In order to take in account this effect, the weight coefficients are adopted to define the linear expansion due to AAR, as proposed by Saouma and Perotti [3]. The linear expansion, ε^i_{AAR} , along the *i-th* principal stress direction is defined as:

$$\varepsilon^i_{AAR} = w_i \ \varepsilon^{vol} \qquad i = 1,2,3 \tag{2}$$

where ε^{vol} is the volumetric expansion defined in accordance with the kinetic law, w_i is the weight for the *i-th* principal stress direction.

The three weights for a generic stress situation are defined as linear interpolation from four specified "nodal" values:

$$w_i = \sum_{j=1}^{4} N_j(\sigma_I, \sigma_{II}) \cdot W_j(\sigma_{III}) \tag{3}$$

where σ_I , σ_{II} are the principal stresses in the plane perpendicular to *i-th* direction and σ_{III} is the principal stresses along *i-th* direction (Figure 3 (a)), W_j are fixed weights defined for sixteen specific situations (Figure 3 (b)), and N_j is the bilinear shape function used in finite element formulations.

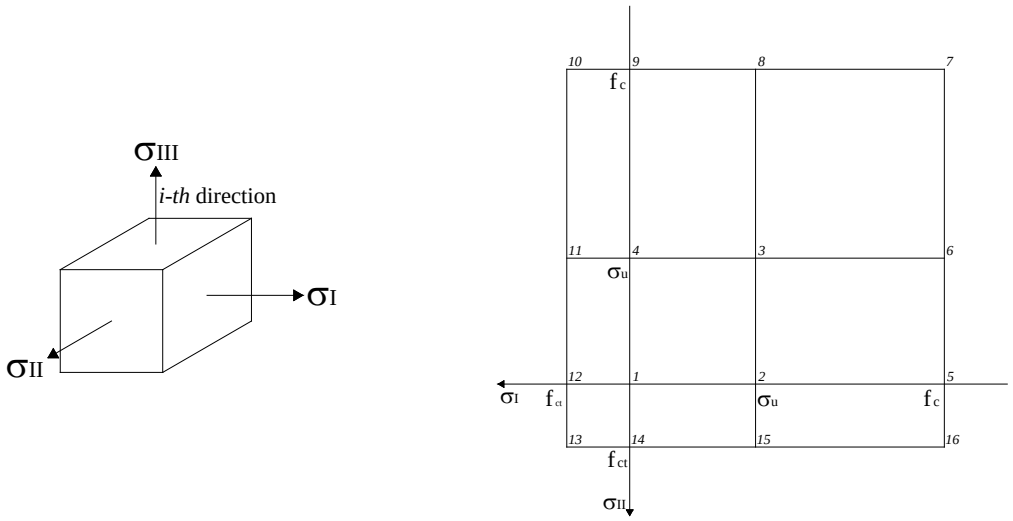

(a) (b)

Figure 3: (a) Principal stresses nomenclature for *i-th* direction; (b) Weight region.

The weight coefficients are defined for a stress range between the tensile strength, f_{ct}, and the compressive strength, f_c, (Figure 3 (b)). On the basis of experimental tests of Struble and Diamond [6], the threshold value σ_u, above which no expansion occurs, is taken equal to -1.0 10^7 N/m^2. Outside the range definition, which is possible in a linear analysis, the weights are considered constant and equal to the values of the nodes on the border line.
Moreover, the weight coefficients along the global axes can be defined with a posteriori formulation:

$$w_k^{XYZ} = \frac{\varepsilon_{AAR}^k}{\varepsilon^{vol}} \qquad k = X, Y, Z \tag{4}$$

where ε_{AAR}^k is the AAR strain along the *k-th* global axis, obtained from the principal AAR strain through the transformation matrix between the principal and global directions.
Based on the to elastic modulus provided in the Benchmark Guidelines [4], the adopted value for the compressive and the tensile strength are chosen equal to -12 10^6 N/m^2 and 1.1 10^6 N/m^2 , respectively.

3. Numerical results

In this Section the numerical results are reported. First, the advanced solution obtained with the model described in the previous section is shown; afterwards the stress influence is further examined through the comparison with simplified methods.

3.1. Advanced solution

In order to make a comparison, measured displacements of nine main instruments (Figure 4), which are clearly related to the swelling phenomenon, are given during 1963-1994 (calibration period).

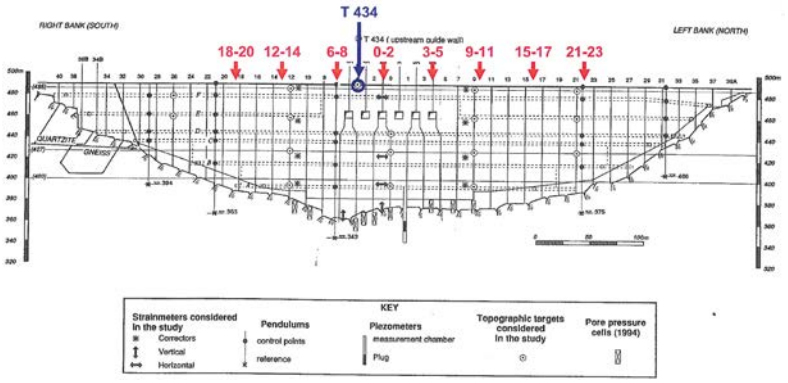

Figure 4: Location of the main instruments [4].

In Figure 5 the comparison between the measured and numerical results is shown. The displacement in radial direction are calculated in a cylindrical reference system with the axis in Z-direction and the origin in the point (0, 230 , 0) m respect to the rectangular coordinate system. Both vertical and radial displacements are obtained by subtracting the initial displacement due to the impounding.

These results derive from a calibration of the kinetic law. The value of the latency time is chosen in agreement with the delay shown in the radial displacement (1962-1975). The value of the characteristic time and the asymptotic expansion are defined in agreement with the vertical displacement at the end of the calibration period (1994).

Figure 6, Figure 7 and Figure 8 show the numerical results of the dam after impounding (1963) and at the end of the calibration period (1994). Each figure gives the stress, the AAR strain and the weights w^{XYZ} for one of the X, Y and Z-directions.

At the end of the calibration period, the swelling redistribution due to the stress state leads to an expansion which varies between 40% and 50% in the Z-direction (w_Z^{XYZ} in Figure 8 (b)). Whereas only 20% of the volumetric expansion occurs is the radial direction (w_X^{XYZ} in Figure 6 (b)). This anisotropic behavior, visible from measurements, can be explained with the "expansion transfer" concept.

Making a comparison between columns (a) and (b) of Figure 6, Figure 7 and Figure 8, it is possible to observe that the expansion influences the internal stress situation and subsequently leads to an evolution of the weights in the time. This aspect confirms the relevance of the swelling redistribution phenomenon. In order to underline this aspect, in the following section a comparison between the advanced solution and simplified method is presented.

Figure 9 and Table 4 give the prediction of the behavior of the dam for 2010.

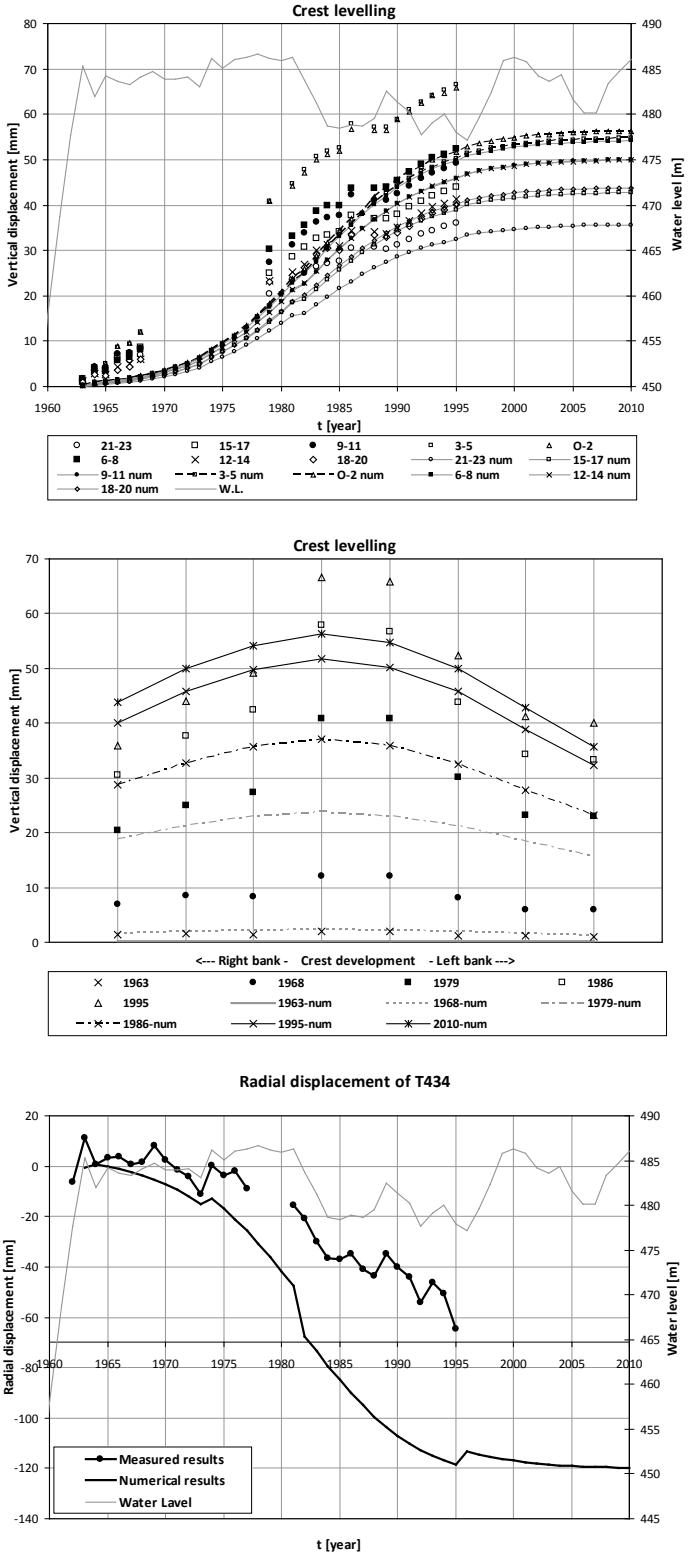

Figure 5: Comparison between measured and numerical results for the advanced solution.

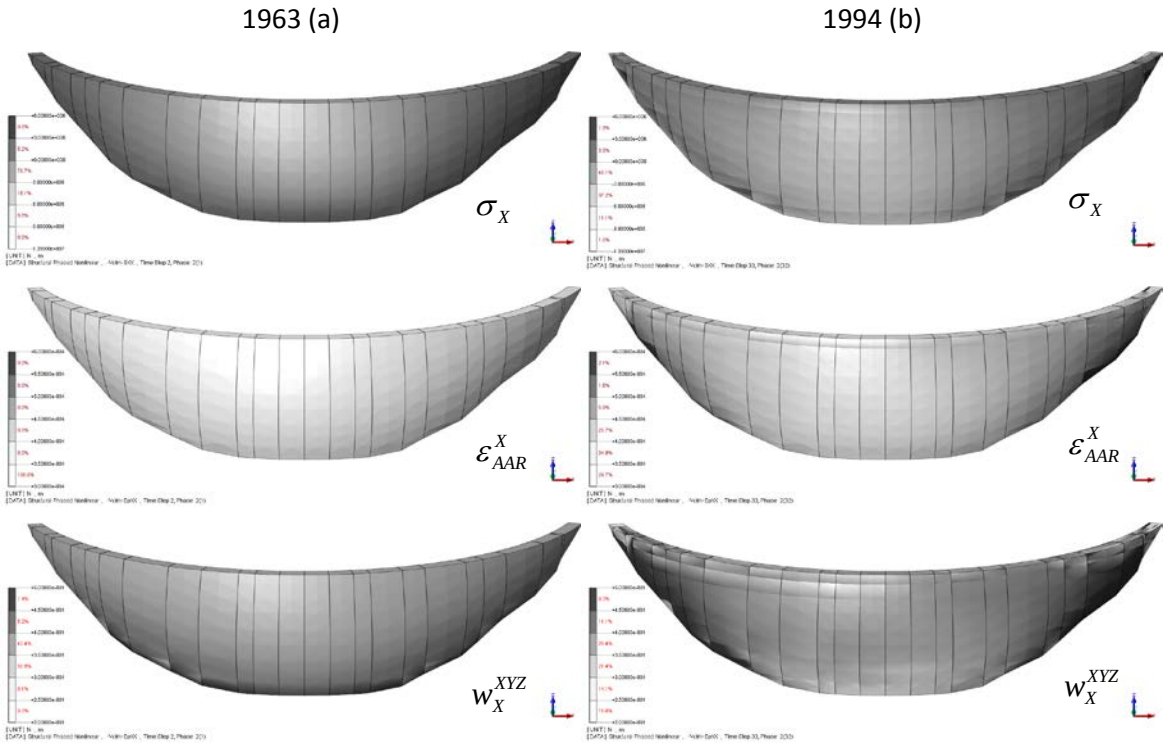

Figure 6: Numerical results along X-axis in 1963 (a) and 1994 (b)

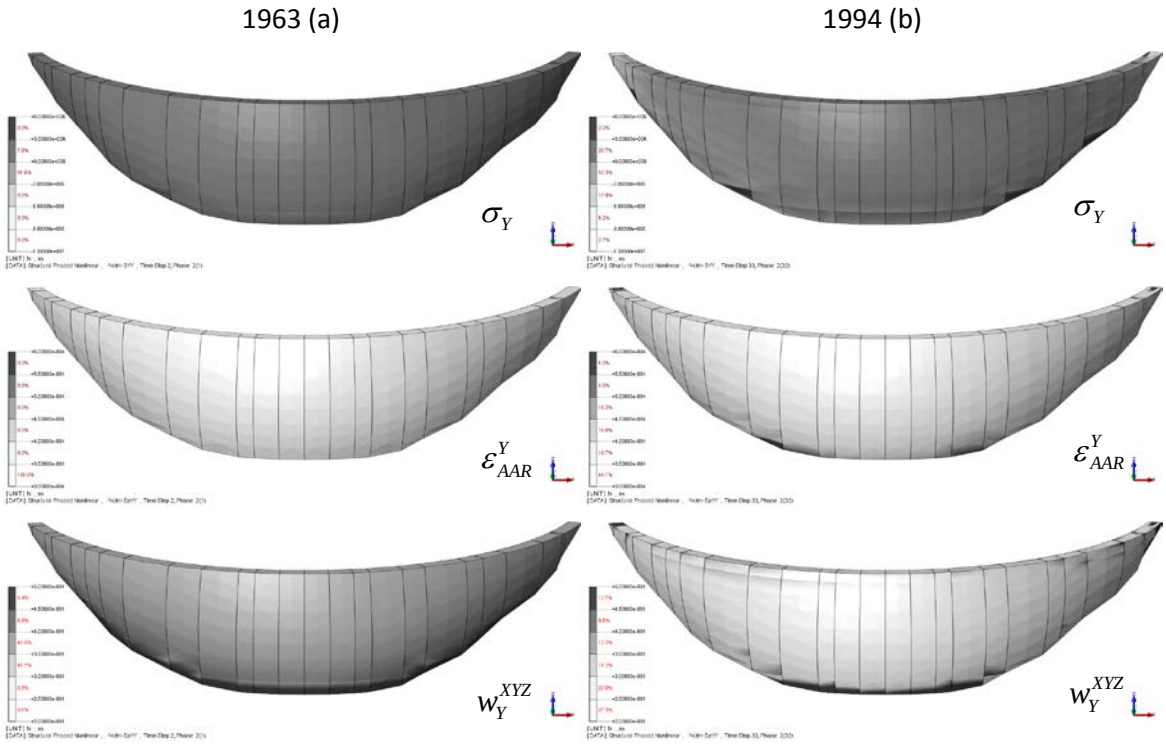

Figure 7: Numerical results along Y-axis in 1963 (a) and 1994 (b)

1963 (a) 1994 (b)

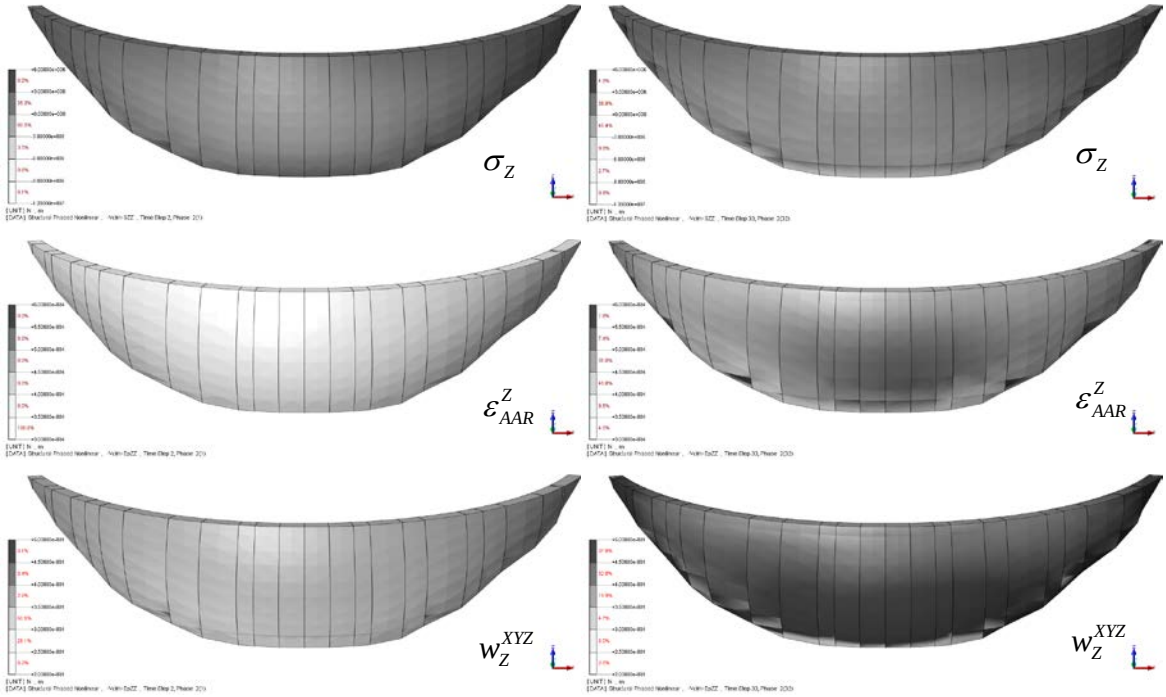

Figure 8: Numerical results along Z-axis in 1963 (a) and 1994 (b)

2010

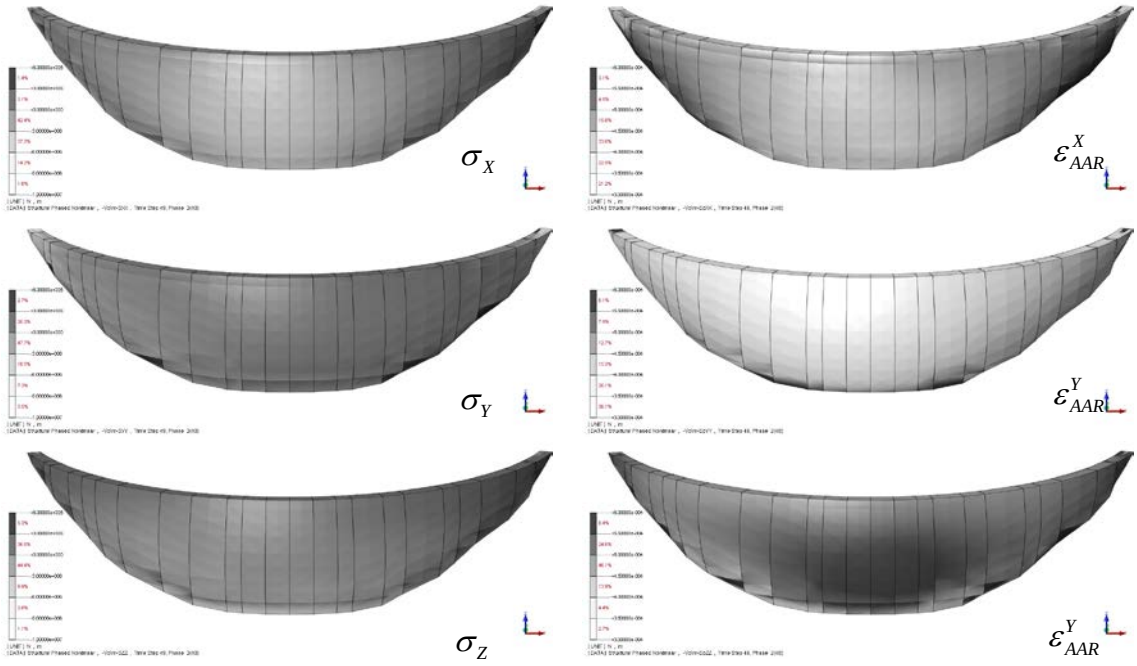

(a) (b)

Figure 9: Prediction of the behavior of the dam for 2010: (a) stress and (b) AAR strain in X, Y and Z-directions.

Table 4: Prediction of vertical and radial displacement of reference point in 2010.

Reference point	Vertical displacement [mm]	Radial displacement [mm]
18-20	43.82	-42.64
12-14	49.97	-80.58
6-8	54.21	-108.28
O-2	56.32	-123.12
3-5	54.73	-115.92
9-11	50.01	-89.06
15-17	42.74	-46.58
21-23	35.63	-7.24
T434	59.12	-119.77

3.2. Relevance of "expansion transfer" concept

In this Section the relationship between stress state and swelling redistribution is underlined. Two straightforward analyses with a priori definition of the weight coefficients in the global coordinate system are given. In the first case, the now fixed and homogeneous w^{XYZ} values are based on the stress situation in the dam after the impounding, in 1963 (column (a) of Figure 6, Figure 7 and Figure 8). Instead, in the second case, they are derived from the stress situation at the end of the prediction period, in 1994 (column (b) of Figure 6, Figure 7 and Figure 8). The volumetric expansion is calculated in accordance with the kinetic law presented in section 2.2 and shown in Figure 2. In
Table 5 the kinetic parameters and the weight coefficients are summarized.

Table 5: Parameters of kinetic law and weights for the two simplified Solutions

Parameter	Advanced solution	Simplified solution 1 (stress state 1963)	Simplified solution 2 (stress state 1994)
Asymptotic expansion ε_∞	0.12 %	0.12 %	0.12 %
Latency time t_l	20 year	20 year	20 year
Characteristic time t_c	5 year	5 year	5 year
w_X^{XYZ}	Stress dependent	0.1	0.35
w_Y^{XYZ}	Stress dependent	0.2	0.2
w_Z^{XYZ}	Stress dependent	0.7	0.45

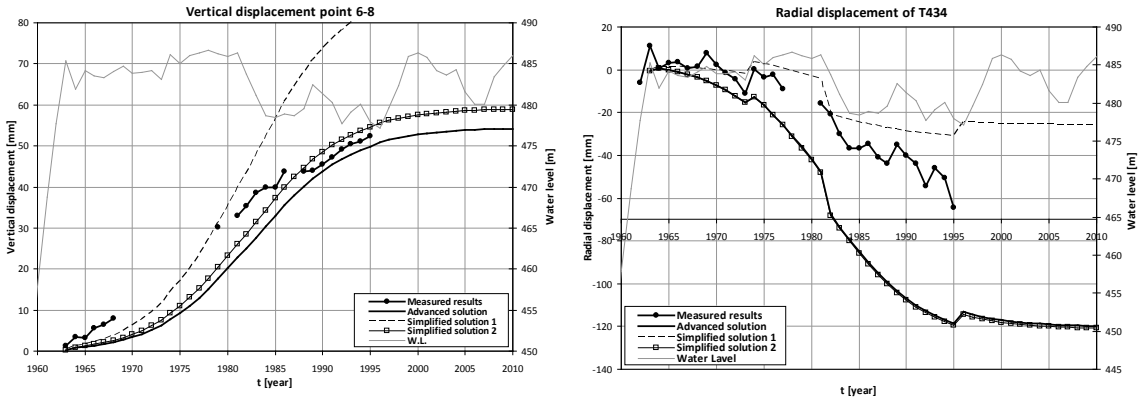

Figure 10: Comparison between the advanced and the two simplified solutions.

In Figure 10 numerical results obtained with the advanced solution and the two straightforward solutions are compared.

For the simplified solution 1, the displacements in both the directions are substantially different from the one obtained with the advanced solution. This means that if the volumetric redistribution is based on the initial stress state a different kinetic law should be selected to obtain a reasonable fitting of the measured results.

The displacement obtained with the simplified solution 2 and the advanced solution are closer. The explanation lies in the source of the stresses: the stresses due to the pressure water remains appreciatively constant, due to the small fluctuation during the service life of the dam, therefore the stresses generate from the AAR expansion play an important role. It is for this reason that if the weight coefficients are calculated in agreement with the final stress state, which includes the AAR expansion, the simplified solution is in agreement with the advanced one.

4. Conclusion

The Kariba dam is adopted as a case study of AAR-affected concrete structures. In this paper a 3D finite element analysis, with a modified version of DIANA software, is carried out in order to predict the behavior of the dam in 2010.

A linear elastic behavior is adopted for the dam and its foundation. Interface elements with nonlinear behavior are introduced between the two components. Rigid tying elements are introduced after the construction phase to simulate the grouting between each cantilever.

The evolution of the AAR swelling in time is defined through the Larive's kinetic law [2]. The calibration of its parameter (asymptotic expansion, latency and characteristic time) takes in account the "expansion transfer" concept with Saouma and Perotti formulation [3].

A comparison between the advanced solution and the simplified solutions is shown in section 4, in order to underline the main role of the stress state on the swelling redistribution.

Acknowledgements

The authors wish to express their thanks to the Dutch Technology Foundation STW for its financial support.

References

[1] Ulm, FJ, Coussy, O, Kefei, L, Larive, C (2000). Thermo-chemo-mechanics of ASR expansion in concrete structures. ASCE Journal of Engineering Mechanics Vol. 126, 3, pp. 233-242.

[2] Larive, C (1998). Apports combinés de l'expérimentation et de la modélisation à la comprehension de l'alcali-reaction et de ses effets mécaniques. Monograph LPC, Laboratoires des Ponts et Chaussées, Paris.

[3] Saouma, V, Perotti, L (2006). Constitutive model for alkali-aggregate reaction. ACI Material Journal, Vol. 103, 3, pp. 194–202.

[4] Noret, C., Molin, X. (2011). Eleventh Internationa Benchmark Workshop on Numerical Analysis of Dams, THEME A, Effect of Concrete swelling on the equilibrium and displacements of an arch dam, October 20-21, Valencia, Spain.

[5] Multon, S, Toutlemonde, F (2006): Effect of applied stresses on alkali-silica reaction-induced expansions. Cement and Concrete Research, (36): 912–920.

[6] Struble, L., Diamond, S. (1981), Swelling Properties of Synthetic Alkali Silica Gels. Jurnal of the American ceramic Society, Vol. 64, 11, pp. 652-655.